Theor. Appl. Climatol. 82, 131–141 (2005)
DOI 10.1007/s00704-005-0125-4

Theoretical and Applied Climatology
Printed in Austria

[1] Nanjing Institute of Geography and Limnology, Chinese Academy of Sciences (CAS), Nanjing, China
[2] Meteorologisches Institut, Universität Hamburg, Hamburg, Germany

Yangtze Delta floods and droughts of the last millennium: Abrupt changes and long term memory

T. Jiang[1], **Q. Zhang**[1], **R. Blender**[2], and **K. Fraedrich**[2]

With 8 Figures

Received March 2, 2004; revised December 6, 2004; accepted January 1, 2005
Published online April 26, 2005

Summary

Climate variability and flood events in the Yangtze Delta, which is a low-lying terrain prone to flood hazards, storm tides and typhoons, are studied in terms of a trend and detrended fluctuation analysis of historical records. The data used in this paper were extracted from historical records such as local annuals and chronologies from 1000–1950 and supplemented by instrumental observations since 1950. The historical data includes frequencies of floods, droughts and maritime events on a decadal basis. Flood magnitudes increase during the transition from the medieval warm interval into the early Little Ice Age. Fluctuating climate changes of the Little Ice Age, which are characterised by arid climate events, are followed by wet and cold climate conditions with frequent flood hazards. For trend analysis, the Mann-Kendall test is applied to determine the changing trends of flood and drought frequency. Flood frequency during 1000–1950 shows a negative trend before 1600 A.D. and a positive trend thereafter; drought frequency increases after 1300. The detrended fluctuation analysis of the flood and drought frequencies reveals power law scaling up to centuries; this is related to long-term memory and is similar to the river Nile floods.

1. Introduction

Climate warming, flood hazards and their impacts on human society have received increasing attention in China during recent years, particularly as agriculture, industry and even the development of national economies suffer losses from flood and water logging hazards (IPCC 2001). The Yangtze Delta is an extremely densely populated and economically developed area with Mega-cities such as Shanghai, Nanjing, and Hangzhou. Shi (2003) and Zhang et al. (2001) show that changes of flood occurrences may reflect climate transitions. Therefore, understanding the principles governing flood occurrence is theoretically and practically meaningful for local mitigation and the reduction of flood induced disasters. A first step towards an understanding of the underlying processes is the analysis of floods and climate change in the past. Research on past climatic fluctuations in China (An, 1986; Wang et al., 1991; Zhang et al., 1995; Gong and Harneed, 2000; James et al., 2000; Zhang et al., 2001) has identified abundant historical records and exceptional information, which is a valuable historical heritage to the study of climate variability. Documentation of Yangtze Delta floods is based on relatively complete and long historical records of climatic events and human activities. Historical records (Zhang et al., 2002) indicate that the Yangtze Delta is typical for the lower Yangtze River in both its geomorphologic characteristics and climatic change patterns. In this study, the historical records are extended by instrumental observations of precipitation, temperature and discharge available from 1950 to 2002.

The analysis presented here is an extension of ongoing research on China's water cycle and climate. Commencing with an in-depth description of the quantification of historical climate data and its transfer into quantitative time series (Wang et al., 1991), the necessary next step was to demonstrate historical climate variability. Fluctuations of flood and drought indicators, which characterise the eastern parts of China, were analysed (by wavelet methods) to identify water cycle related regimes over the past millennium (Jiang et al., 1997). Based on instrumental precipitation records, a novel monitoring algorithm, the standardised precipitation index (SPI), was introduced (Bordi et al., 2004). Thus, a unique set of analyses has been accomplished, ranging from historical data extraction and climate variability analysis to monitoring and practical prediction of wetness/drought regimes. These analyses will be extended with the application of a novel nonlinear systems analysis technique used to detect long term memory as an underlying mechanism for water cycle variability in eastern China, in particular, in the Yangtze Delta area.

First steps towards analysing regional climate variability are commonly associated with climate change, which is described and quantified in terms of internal fluctuations manifested in power spectra or similar methods. An example of these methods is the detrended fluctuation analysis (DFA), which has been developed recently (Peng et al., 1994) to extract the scaling properties of the fluctuations and thereby to characterise the complex dynamics underlying climate variability. This analysis technique has been applied systematically to temperature time series of last century observations and of coupled global ocean-atmosphere circulation models (Fraedrich and Blender, 2003, loc. cit.). The time scales resolved by this method are, due to sampling, limited by about a tenth of the length of the time series. Beyond that, trend analysis is used to identify an abrupt climate change in the time series. The millennium time series of Yangtze Delta floods provides an ideal testbed for the application of both the established and novel methods to gain insight into the underlying dynamics *and* to provide appropriate measures for comparison with climate models simulating both control (trend-free) and close to reality (trend) situations.

We describe the climatological embedding and the data sets to be analysed (Section 2) followed by the methods applied (Section 3). The results for the historical climate, trends and long term memory are presented in Section 4 and summarised in Section 5.

2. Climatological setting and data

The Yangtze Delta (30° N to 33° N, 119° E to 122° E) is located in Eastern China and characterised by the subtropical monsoon climate (Fig. 1). Mixed deciduous and evergreen forest determines the natural vegetation of the region. The mean annual temperature is 15.5 °C. In summer, the area is dominated by the Subtropical High with maximum temperatures reaching 28.9 °C; in winter, the region is influenced by the Mongolian High with minimum temperatures around 3.3 °C. The mean annual precipitation is 1235 mm with summer rainfall (June–August) accounting for 40% of the total and only 11% occur during winter months (December–February). Climatologically, the region is sensitive because it lies along the demarcation between subtropical and temperate climates characterised by significantly disparate air masses (Daniel et al., 1996). Thus, it is affected by maximum floods that

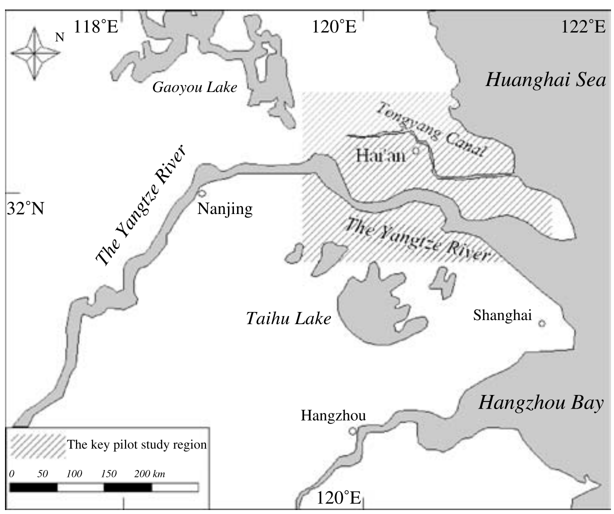

Fig. 1. The Yangtze Delta with the key pilot study region (shaded)

mostly result from excess rainfall during summer, especially June and July (the so-called Plum Rainy Season) when slow-drifting cold fronts encounter moist air masses of subtropical origin and also in August which is characterised by typhoon-induced excessive precipitation. A nearly level plain with an elevation of 2 to 7 m above sea level covers 75% of the region. This low-lying terrain makes the region vulnerable to floods, maritime tidal and other natural hazards (Daniel et al., 1996). In addition, low-lying terrain causes retarded discharge of ground surface water and therefore, excessive precipitation usually results in floods. The Yangtze Delta is a well-developed area in industry and agriculture and densely populated with sufficient historical and instrumental climatological data available.

The information used for our analysis are annual time series characterising flood and drought occurrence of the middle Yangtze and the Yangtze Delta for the period 1000 to 1950. The data base consists of historical documents (1000–1950, Hu and Luo, 1988 and MICMB, 1981) from which quantitative information can be extracted. A grading, $G(t)$, is used for each year t during the last millennium to establish a time series, which characterises individual flood ($G = -2$ and -1 for heavy flood and flood),

Table 1. Frequency of the floods, drought events, maritime tidal events (Number of natural hazards per ten years) extracted from historical documents

Year	Flood	Drought	Maritime events	Year	Flood	Drought	Maritime events	Year	Flood	Drought	Maritime events
1005	1	2	0	1365	0	0	0	1715	3	3	0
1015	0	3	1	1375	0	0	1	1725	0	1	2
1025	4	0	0	1385	1	0	1	1735	4	1	3
1035	0	3	0	1395	0	1	1	1745	4	1	1
1045	0	2	0	1405	1	0	0	1755	3	2	2
1055	0	0	0	1415	1	0	0	1765	1	1	0
1065	1	0	0	1425	0	1	1	1775	1	3	1
1075	0	2	0	1435	1	3	0	1785	1	5	0
1085	2	1	0	1445	4	1	0	1795	0	1	3
1095	1	0	0	1455	4	1	0	1805	1	7	3
1105	1	3	0	1465	2	1	1	1815	2	3	0
1115	3	2	0	1475	1	3	0	1825	3	1	0
1125	0	1	0	1485	0	5	0	1835	5	2	0
1135	1	5	1	1495	1	0	0	1845	2	1	1
1145	0	2	0	1505	0	5	0	1855	1	3	2
1155	2	1	0	1515	2	3	2	1865	1	2	1
1165	0	1	0	1525	3	4	1	1875	1	5	0
1175	0	0	1	1535	2	3	1	1885	2	1	1
1185	0	4	0	1545	2	2	0	1895	0	3	0
1195	2	3	0	1555	4	4	0	1905	4	0	0
1205	5	4	0	1565	7	1	0	1915	3	2	0
1215	1	2	0	1575	9	0	0	1925	1	4	0
1225	1	0	0	1585	4	2	2	1935	1	3	0
1235	0	0	0	1595	6	0	0	1945	1	0	0
1245	0	2	0	1605	3	1	0	1950	2	0	3
1255	0	0	0	1615	4	4	0	1955	1	1	1
1265	0	0	0	1625	3	2	0	1960	1	1	0
1275	0	0	1	1635	4	6	0	1965	2	2	0
1285	2	0	0	1645	1	3	1	1970	2	3	0
1295	2	3	0	1655	2	5	1	1975	2	2	0
1305	1	1	0	1665	3	1	3	1980	2	2	1
1315	0	0	1	1675	7	2	0	1985	2	3	1
1325	1	2	2	1685	1	1	0	1990	0	2	1
1335	0	2	1	1695	4	0	0	1995	2	3	1
1345	0	0	1	1705	3	1	0	2000	4	2	2
1355	0	0	0								

normal ($G = 0$), and drought (drought and heavy drought, $G = 1$ and 2) events, hence $G(t) = -2, -1, 0, 1, 2$. For example, "1335, tidal inundation occurred accompanying floods, many people died" (2-grade flood), "1512, July, it is windy, tidal inundation occurred. Houses and people were damaged and in inundation in thousands" (1-grade flood), "1539, tide level rose rapidly, the depth of the ground surface water is tens of meters, thousands of people died" (1-grade flood). Some historical records indicate that floods are partly a direct result of tidal events.

Here we use frequency statistics derived from the grade time series $G(t)$, to make it comparable with other millennium data and define decadal flood and drought events F and D (Table 1). Droughts are defined by $d(t) = 1$ for $G > 0$, and floods, $f(t) = 1$ for $G < 0$. These yield the decadal sums $D(t_c) = \Sigma_t d(t)$ and $F(t_c) = \Sigma_t f(t)$ for the decadal times t_c during the last millennium, $t_c = 1005, 1015, 1025, \ldots$, and the years involved in the sums are $t = t_c + (-5, -4, \ldots, +4)$. In addition, the number M of marine tidal events per decade is extracted from historical documents in a similar manner (Table 1). Finally, a humidity parameter I is introduced (Zheng, 1997), which depends on the decadal frequencies of floods and droughts, F and D (published in MICMB, 1981, see Table 1)

$$I = 2\frac{F - D}{F + D} \tag{1}$$

If the occurrences of flood and drought events are equal, $I = 0$ (also if no flood and drought events are measured); if the climate is wet or dry, $I > 1$ or $I < 1$. The decadal time series of floods, drought and maritime events, D, F, M, and the humidity index, I, are subjected to trend and detrended fluctuation analysis.

Table 2. The flood/drought grade criteria for instrumental precipitation data (1950–2002) in the Yangtze Delta. R_i is the precipitation at each station in the Yangtze Delta from May to September since 1950, $\bar{R}$ the multi-year average precipitation and σ is the standard deviation (MICMB, 1981)

Index	Grade	Type
$R_i > (\bar{R} + 1.17\sigma)$	2	Heavy flood
$(\bar{R} + 0.33\sigma) < R_i \leq (\bar{R} + 1.17\sigma)$	1	Flood
$(\bar{R} - 0.33\sigma) < R_i \leq (\bar{R} + 0.33\sigma)$	0	Normal (harvest year or missing records)
$(\bar{R} - 1.77\sigma) < R_i \leq (\bar{R} - 0.33\sigma)$	-1	Drought
$R_i \leq (\bar{R} - 1.77\sigma)$	-2	Heavy drought

The historical data are complemented by instrumental observations after 1950 based on the NCEP reanalysis data set (Kalnay et al., 1996). The grades $G(t)$ during the instrumental period are determined by the precipitation using the criteria in Table 2. An SST (sea surface temperature) index is used which characterises El Nino/Southern Oscillation events (COAPS, 2004). This index is defined as the 5-month running mean of the monthly SST anomalies averaged over the areas 4° N to 4° S and 150° W to 90° W.

3. Analysis methods

Two methods are applied to determine climate change and low frequency variability in the historical and instrumental data: (1) The detection of trends and trend changes is performed by the Mann-Kendall-test, a rank-test that determines a single trend change in a time series. (2) The low frequency variability is determined by the detrended fluctuation analysis, an extension of the fluctuation analysis with the particular capability to investigate long time memory in time series. These methods of analysis are described below.

3.1 Abrupt changes: Mann-Kendall test

Abrupt changes and trends of floods and maximum summer temperatures are diagnosed by the Mann-Kendall rank test (MK, as suggested by Sneyers, 1975; Goossens and Berger, 1987). This technique has been applied to dryness (in China, Jiang and Qian, 1997) and to flood levels (Nile river, Fraedrich et al., 1997, see also Jiang et al., 2002).

Estimating abrupt changes using the Mann-Kendall test (MK) is based on a progressive analysis to test the beginning of a single trend (within a given sample time series) utilising related progressive and retrogressive rank series. MK is suitable to detect one abrupt change in a sample time series of anomalies that are independent and Gaussian distributed. First, assume that the time series is in progressive sequence, $x_1, x_2, x_3 \ldots x_N$ for a given sample size N. The accumulated total of values x_j smaller than x_i

for $j<i$ up to i is denoted as m_i. The sum of the first of these terms is the rank statistic d_k

$$d_k = \sum_i^k m_i, \quad \text{for } k = 2, \ldots, N \tag{2}$$

This sum is standardised to a normal distribution by

$$Z_1(k) = \frac{d_k - E[d_k]}{\sqrt{\text{var}[d_k]}} \tag{3}$$

with the mean $E[d_k] = k(k-1)/4$ and the variance $\text{var}[d_k] = k(k-1)(2k+5)/72$.

A trend of the time series is significant at the threshold U_a if $Z_1(k) > U_{\text{a}}$. For the standard significance level $a = 0.05$ the threshold is $U_{0.05} = 1.96$. To identify an abrupt climate change, this analysis is performed with the same time series but with the retrograde sequence, i.e. $x_N, x_{N-1}, \ldots, x_1$, and yields $Z_1(k) = -Z_2(k)$ for $k = N, N-1, \ldots, 1$. An abrupt change is initiated at the intersection $Z_1(k)$ and $Z_2(k)$.

3.2 Long term memory: Detrended fluctuation analysis (DFA)

Long term memory is a particular case of enhanced low frequency variability when the time integral of the auto-correlation function diverges. Due to this, the correlation time is infinitely large. In practice, due to the finite range of any observed or modelled time series, long term memory is considered to exist if there is no exponential decay up to the maximum time scale. The detrended fluctuation analysis (DFA) has been developed to determine the variability of time series on different time scales (Peng et al., 1994) and is becoming an ideal tool to derive long term memory (e.g. Fraedrich and Blender, 2003). The DFA determines the fluctuation function $F(t)$, however, and this is the difference to the standard fluctuation analysis, for the integrated time series, the so-called profile. The effect of the integration is reversed after the calculation. For this profile, linear fits are determined for all segments of different widths t and the fluctuation function $F(t)$ is calculated as the standard deviation between the profile and the time series. The main advantage of the DFA is that long time correlations become visible by the integration. For scaling behaviour, which shows up as a power law in $F(t)$, there are direct relationships to the correlation function and the power spectrum of the time series: if $F(t) \sim t^{\alpha}$ the power spectrum follows $S(f) \sim f^{-\beta}$ with $\beta = 2\alpha - 1$, and the correlation function is $C(t) \sim t^{-\gamma}$ with $\gamma = 1 - \beta$. The exponent α equals the Hurst exponent (1951) obtained by the rescaled range analysis. Stationary long term memory is present within $0 < \beta < 1$ $(1/2 < \alpha < 1)$. The two limiting cases are uncorrelated time series (white noise) with $\beta = 0$ $(\alpha = 1/2)$ and the $1/f$-spectrum (flicker noise) with $\beta = 1$ $(\alpha = 1)$. For $\beta > 1$ $(\alpha > 1)$ the time series is non-stationary and conventional statistical analysis cannot be applied. In the case of dominant oscillations the fluctuation function $F(t)$ shows step-like transitions at the oscillation periods, and hence, the result may be difficult to interpret for a multitude of oscillations. Therefore, the DFA should be combined with a power spectrum analysis.

The DFA analysis, which does not – in contrast to its name – eliminate trends in the data, can be extended to higher order versions DFA-N, which fit and subtract higher order polynomials of degree N to the profile (DFA-1 represents the standard DFA). In order to avoid any confusion with the trend analysis above, it is necessary to differentiate the time scales involved. For DFA-N the time scales of interest are well below the total available duration of the time series since the same conditions for significance as for a power spectrum apply. Therefore, the time scale of the polynomials subtracted in DFA-N is below about 100 years. On the other hand, the trend analysis, which is another main topic in the present study, is applied to climate changes on the centennial time scale. The essential result of the DFA is the decadal variability and thus complements the Mann-Kendall analysis.

4. Results: Climate history, trends and long term memory

The historical data are decadal flood and drought frequencies during the last millennium (from these a humidity parameter is derived) and the instrumental data precipitation, temperature and the SST index characterising the El Nino/Southern Oscillation (COAPS, 2004). They are analysed in three steps: First the historical and instrumental data time series are presented with an overview of wet and dry periods. Then, a Mann-Kendall trend analysis is applied to the historical and instrumental data, and finally, the long term memory is determined in the historical data.

4.1 The historic and instrumental data

Historical data: Figure 2 demonstrates the connections between flood events, climatic changes and maritime tidal events. Eight frequently-occurring flooding periods are marked as the shaded zones a–h. A time interval during 1500 and 1800, which is characterised by a high frequency of floods, is the Little Ice Age (see, for example, Bradley et al., 1992; Huang, 2000; Yang et al., 1995). In our key region the Little Ice Age is characterised by high wetness, $I>1$, with alternating wet and dry climate episodes. Larger floods are noted from 1500 to 1700, which characterises the transition from the medieval warm interval to the cooler Little Ice Age (temperatures taken from Wang et al., 2002). The same transition occurred in the upper Mississippi River (James, 1993). It can also be seen from Fig. 2 that the occurrences of maritime tidal and flood events are correlated. As these eight shaded zones show, periods with tidal events and floods occurred almost simultaneously (except zone a and zone b), the maritime tidal events had a more significant impact on the occurrence of the floods in the Yangtze Delta than other more direct effects. The low-lying terrain makes the study region prone to impacts of floods and extreme tides. Figure 2 also demonstrates that drought and flood events usually occurred concurrently.

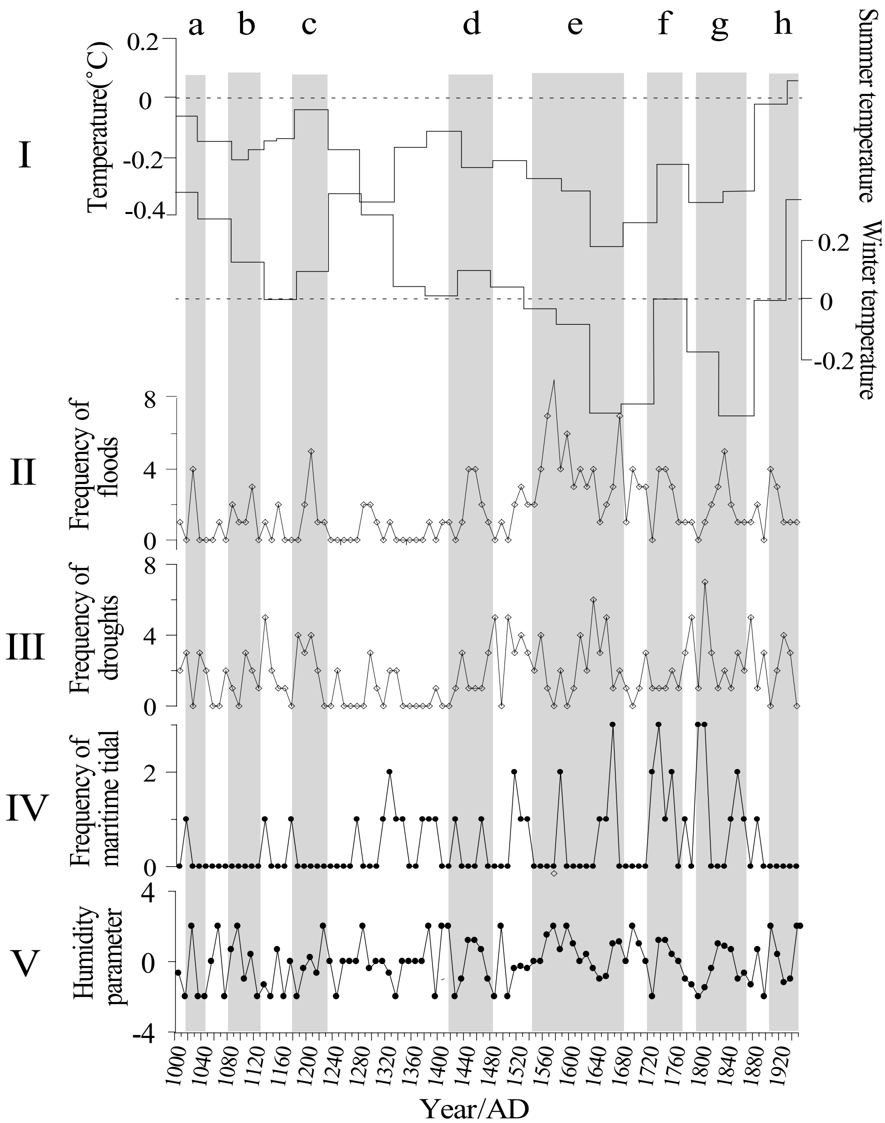

Fig. 2. Flood events, tidal events and temperature changes evolving in the Yangtze Delta. The dashed lines in panel IV and V denote the 50-year moving average, in panel I they denote zero degrees. The shaded zones mark periods of higher-frequency floods (the data are listed as the appendix) coinciding with climate changes of China (Wang et al., 2002)

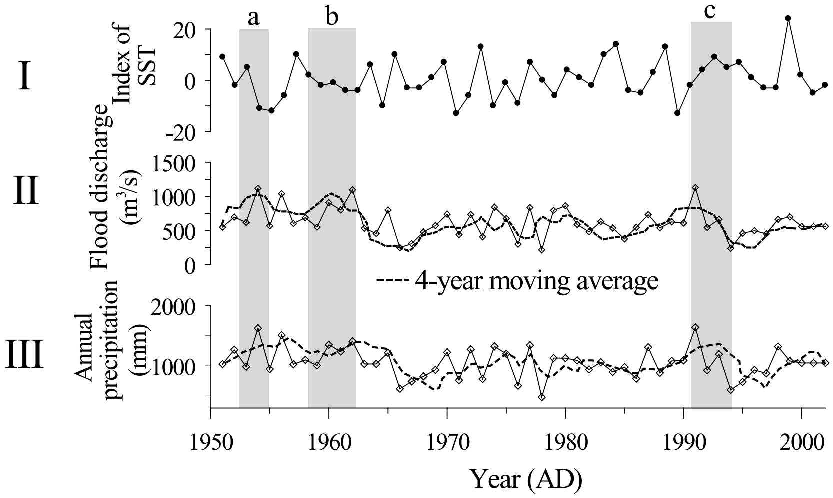

Fig. 3. Mean sea surface temperature (SST) index, flood discharge, and annual precipitation in the lower reaches of the Yangtze River from instrumental records (1950 to 2002); discharge with 4-year moving average (dashed) of rivers in the Yangtze Delta

We can see that these eight flooding periods are also the drought periods (flooding events and drought events occurred at the same year, e.g. the flood events occurred in the spring and the drought event occurred in the autumn). It should be mentioned here that the connections between flood events and tidal inundation are not significant, because tidal inundation events are not the decisive cause of flood occurrence.

Instrumental data: Close connections between annual precipitation, flood discharge and SST index, demonstrated in Fig. 3, occur in certain periods marked by shading. This may be the reason why correlations between SST, annual precipitation and discharge are not significant. These three shaded zones (Fig. 3) show three periods, which are characterised by greater flood discharge (see 4-year running mean). Figure 3 also indicates that these three periods correspond to higher mean SSTs. These three periods (shaded zones) also match the frequently-occurring periods of floods in the lower Yangtze River. Therefore, we can tentatively draw the conclusion that higher SSTs appear to enhance the hydrological cycle linking ocean and continent, with excessive precipitation and the increasing possibility of larger floods. Figure 4 shows correlations between the annual precipitation and flood discharge of the Yangtze Delta, with linear connections between flood-season discharge (averages from June to September) and annual precipitation. The regression fit is high ($R^2 = 0.87$) and demonstrates significant impacts of precipitation on floods in the study region.

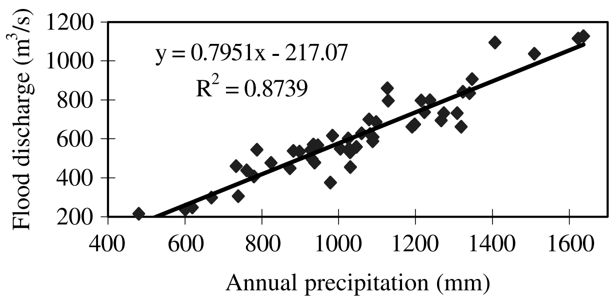

Fig. 4. Correlation between annual precipitation and the flood discharge during 1950–2002 at a tributary river basin of the Yangtze Delta

Flood-season discharge, annual precipitation and SST index: The Pearson correlations between SST index and annual precipitation and discharge is weakly positive. A highly significant correlation of 0.935 exists between annual precipitation and discharge (two-tailed significance at 99%). Note that a general characteristic of the monsoon climate is the strong correlation between precipitation and floods in the rainy summer season (June to August).

4.2 Trend analysis of historical and instrumental data

The Mann-Kendall outcome is presented in Fig. 5. The historical sample (1000 to 1950) shows a negative trend in flood frequency before 1600 (Z_1 curve, at 95% significance) and a weak positive trend thereafter, from 1600 to 1950. The discontinuity of the trend in flood frequency occurs around 1550 (95% significance). For drought frequency a positive trend is found from 1400

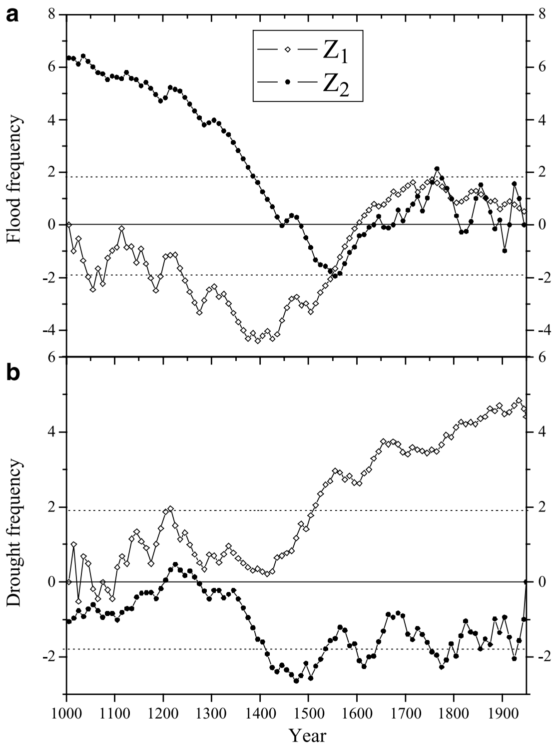

Fig. 5. Mann-Kendall analysis results of the flood frequency (**a**) and drought frequency (**b**) during 1000–1950 in the Yangtze Delta. The two dashed lines denote the 95% confidence level

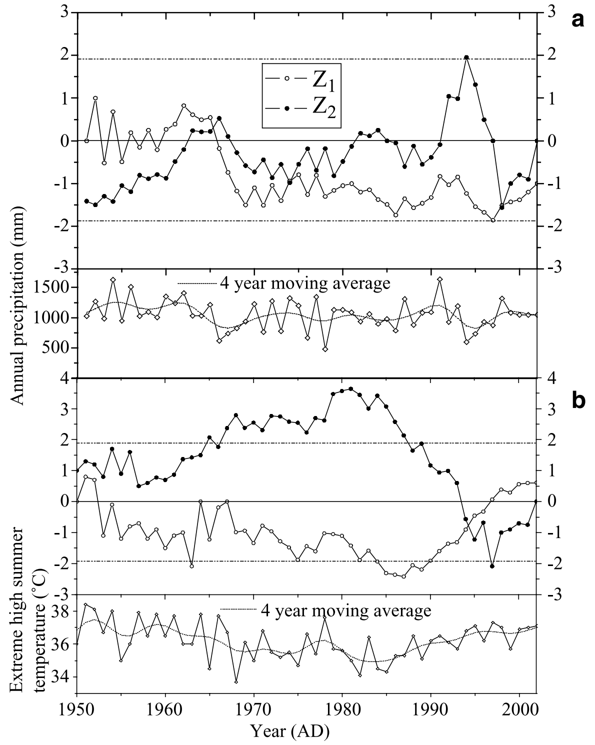

Fig. 6. Mann-Kendall analysis result of the annual precipitation (**a**) and that of the extreme high summer temperature (**b**) during 1950–2002 in the Yangtze Delta. The two dashed lines denote the 95% confidence level

(Z_1 curve) until present-day, however we do not detect a discontinuity in the time series.

In the instrumental sample (Fig. 6) an abrupt change in the annual precipitation time series occurs in the mid 1960s (passing the significance level of 95%). The Z_1-curve demonstrates a negative tendency in the summer precipitation (also passing the 95% level). After the 1970s, precipitation changes are negligible.

However, looking at the fit line with negative slope, the general trend of annual precipitation is negative. The original annual precipitation curves (Fig. 6a) demonstrate this negative trend after 1990. Figure 6b indicates that the discontinuity of the trend of the maximum summer temperature is in the mid 1990s, around 1993. The Z_1-curve demonstrates that the maximum summer temperature changes follow a negative trend before 1990s and positive trend after the 1990s (satisfying a 95% significance). This changing point can be seen in the 4-year moving average curves (Fig. 6b). While the flood frequency shows a negative trend before the 1990s, a positive tendency is found after the 1990s, which matches the maximum summer temperatures of the study region. This suggests an increasing probability of maximum summer temperature (under climatic warming scenarios, James, 2000; Mirza, 2002; Deng et al., 2000), which may lead to an increasing occurrence of flood events.

4.3 Long term memory of historical data

The frequencies of floods, droughts and the deduced humidity parameter Eq. (1) are subjected to DFA to determine the functional relationship of the long term memory. For the duration of 1000 years, results in the time range up to 100 years can be reliably derived. Figure 7 shows the fluctuation functions in a log–log-plot where power laws follow straight lines. Floods and droughts reveal power law exponents α above $1/2$ which represent long term memory up to different time scales: 200 years for floods and without restriction for droughts. The exponents are $\alpha = 0.69$ ($\beta = 0.38$) for droughts and $\alpha = 0.76$ ($\beta = 0.52$) for the frequency of floods. These results have been compared with the

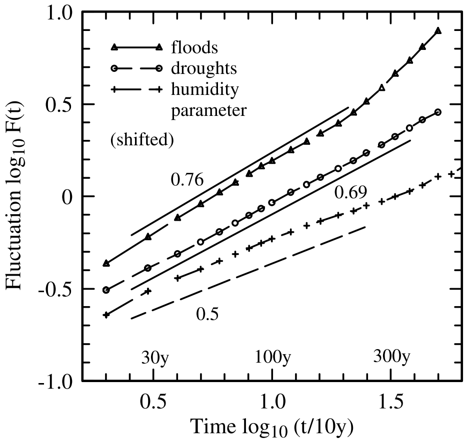

Fig. 7. Fluctuation functions $F(t)$ for the decadal time scale t for floods (Δ), droughts ($\circ$), and the humidity parameter ($+$) obtained by DFA. The lines describe power laws with exponents α as indicated

higher order DFA-2 and DFA-3 to elucidate the role of superimposed linear and quadratic trends on time scales below 100 years: both methods (not shown) reveal the analogous power laws and the exponents agree with DFA-1 findings. Note that the trends investigated in the preceding section are determined above this time scale. A possible origin for the long term memory of the hydrological cycle in this region is the sea surface temperature of the East China Sea. The humidity parameter shows a white spectrum ($\alpha = 0.5$, $\beta = 0$) and no long term memory. The most probable reason is that, by its definition Eq. (2), the long term memory effects of floods and droughts may be obscured.

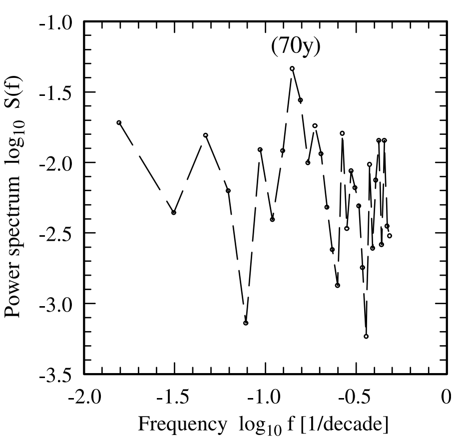

Fig. 8. Power spectrum $S(f)$ for spectral frequency f of the maritime events with the maximum intensity at 70 years. $S(f)$ is averaged in three non-overlapping segments of the total time series

The frequency of maritime events shows a different outcome for the long term variability. Maritime events are rarely found before 1300 A.D. which reduces the total variability and the significance of the results. According to a power spectrum analysis (Fig. 8, determined as an average of three disjoint segments) an oscillation with a period around 70 years may exist, however, this remains speculative in the available time range. The overall behaviour of the power spectrum hints to an absence of long term correlations. Due to the presence of the oscillation the DFA fluctuation function (not shown) cannot reveal a power law behaviour and, from this point of view, the question of long term variability in the frequency of maritime events remains unsettled.

5. Summary and conclusions

Yangtze Delta flood data covering up to a 1000 years are analysed in terms of trend changes and low frequency variability in the range of decades to centuries. Rapid and strong fluctuations of the climate (frequent changes of wet and arid conditions) occur during the Little Ice Age (1500 to 1850, see Bradley, 1992) with frequent flood events in the Yangtze Delta. Larger floods occurred from about 1500 to 1700 and characterise the transition from the medieval warm episode to the cooler Little Ice Age (similar to the upper Mississippi River (James, 1993)). The low-lying terrain of the study region means that flood tides are an important contributor to floods events. Indeed, according to historical records, some floods are the direct result of flood tidal events. This result appears to be beneficial when considering future mitigation and flood hazard reduction for the Yangtze Delta.

Analyses of abrupt changes and trends in the historical records indicate that, during 1000 to 1950, the flood frequency reveals a negative trend before 1600 A.D. and a positive trend thereafter (from 1600 to 1950, but not at 95% significance); from 1700 to 1800 this trend is positive with 95% significance. Instrumental records of annual precipitation indicate an abrupt change occurred in the 1990s. Prior to this, annual precipitation shows a negative trend, whilst post-1990s the discharge trend reverses to become positive. Similarly, the maximum monthly summer temperatures show an abrupt change in the mid 1990s. The $Z_1(k)$ curves of annual precipitation and maximum temperature series show a negative trend before 1990s and positive trend after 1990. Deng et al. (2000) suggest that climatic warming may lead to a high occurrence probability of maximum summer temperatures. Based on the close relationship between changes in annual precipitation and the maximum summer temperature, leads us to surmise that maximum summer temperatures may be greater in the future under a warming scenario, due to the anticipated increases in serious summer rainfall. Still, flood control remains an arduous political and engineering problem which requires serious consideration if future climatic warming is expected for the Yangtze area. Pearson correlation analysis indicates that close connections occur between annual precipitation, flood discharge and mean SST (99% level). Therefore, external forcing, that is changing SSTs, may be helpful in estimating future flood hazard probabilities.

The detrended fluctuation analyses of the flood and drought fluctuations show long term memory with a power law scaling. The estimated power law exponents for the millennium data set are distinctly different from white noise and yield the related spectra $S(f) \sim f^{-0.5}$ for the flood frequency and $S(f) \sim f^{-0.4}$ for the drought frequency. The long term memory extends at least up to 100 years and appears not to be restricted by the total available millennium time range for the flood frequency. The frequencies of the maritime events however, indicate a period of 70 years and long term correlation cannot be proven. The most likely reason for the observed long term memory is the sea surface temperature of the adjacent East China Sea which delivers warm and moist air during the monsoon phases.

Acknowledgements

This paper is financially supported by the key project of Chinese Academy of Sciences (KZCX3-SW-331), Preparation grant of the Nanjing Institute of Geography and Limnology, CAS (No. SS220007), National Natural Science Foundation of China (Grant No. 40271112), National Postdoctoral Research Programme of China and the K. C. Wong Education Foundation, Hong Kong. We also would like to thank the National Climate Centre of China Meteorological Agency to provide us the instrumental data. We should extend our thanks to Prof. Chen Jiaqi in the Nanjing Institute of Geography and Limnology, CAS, for providing part of valuable historical data of climatic changes of the study region. The support by the Deutsche Forschungsgemeinschaft (FR450) is acknowledged.

References

An ZS (1986) Environmental variation of past 20000 years of China. In: Liu TS, An ZS (eds) Loess Global changes. Beijing: Science Press, pp 1–26 (In Chinese)

Bordi I, Fraedrich K, Jiang J, Sutera A (2004) Fluctuations and patterns of dry and wet periods: Eastern China. Theor Appl Climatol 79: 81–91

Bradley RS, Jones PP (eds) (1992) Climate since A.D. 1500. London: Routledge, pp 1–31

COAPS (2004) ENSO Index According to JMA SSTA, Center for Ocean-Atmospheric Prediction Studies, ftp://www.coaps.fsu.edu/pub/JMA_SST_Index

Daniel JS, Chen ZY (1996) Neolithic settlement distribution as a function of sea level-controlled topography in the Yangtze delta, China. Geology 12: 1083–1086

Deng ZW, Ding YG, Chen YG (2000) Influences of global warming on the occurrence probability of the maximum summer temperature in the Yangtze Delta. Journal of Nanjing Institute of Meteorology 23(1): 42–47 (In Chinese)

Fraedrich K, Jiang J, Gerstengarbe FW, Werner PC (1997) Multiscale detection of abrupt climate changes: Application to Nile river flood levels. Int J Climatol 17: 1301–1315

Fraedrich K, Blender R (2003) Scaling of atmosphere and ocean temperature correlations in observations and climate models. Phys Rev Lett 90: 108501

Goossens C, Berger A (1987) How to recognize an abrupt climate change? In: Berger WH, Labeyrie LD (eds) Abrupt climate change, evidence and implications. NATO ASI series C: Mathematical and Physical Sciences, Vol. 216. Dortrecht: D. Reidel, pp 31–46

Hu MS, Luo CZ (1988) Chinese historical great flooding events. Beijing: Book Store Press

Huang CC (2000) Climatic changes. Beijing: Science Press, pp 140–156 (In Chinese)

Hurst HE (1951) Long-term storage capacity of reservoirs. Trans Am Soc Civ Eng 116: 770–808

IPCC (Intergovernmental Panel on Climate Change) (2001) Climate Change 2001: The Scientific Basis. Cambridge: Cambridge University Press, 785 pp

James CK (1993) Large increase in flood magnitude in response to modest changes in climate. Nature 361: 430–432

James CK (2000) Sensitivity of modern and Holocene floods to climate change. Quaternary Science Reviews 19: 439–457

Jiang J, Zhang D, Fraedrich K (1997) Historic climate variability of wetness in East China (960–1992): A wavelet analysis. Int J Climatol 17: 969–981

Jiang J, Mendelssohn R, Schwing F, Fraedrich K (2002) Coherency detection of multiscale abrupt changes in historic Nile flood levels. Geophys Res Lett 29(8): 112-(1-4)

Kalnay E et al (1996) The NMC/NCAR reanalysis project. Bull Amer Meteor Soc 77: 437–471

Meteorological Institute of the Chinese Meteorological Bureau (Chief editor) (MICMB) (1981) Atlas of the Flood/Dryness in China for the Last 500-Year Period. Beijing, China: Cartological Press

Mirza MMQ (2002) Global warming and changes in the probability of occurrence of floods in Bangladesh and implications. Global Environmental Changes 12: 127–138

Peng CK, Buldyrev SV, Havlin S, Simons M, Stanley HE, Goldberger AL (1994) On the mosaic organization of DNA sequences. Phys Rev E 49: 1685–1689

Shi YF (2003) Estimation of climatic transition from warm dry to warm moist in the north-western China. Beijing: Meteorological Press, pp 1–120 (In Chinese)

Sneyers R (1975) Sur l'analyse statistique des series d'observation. WMO TN 143, World Meteorological Organisation, Geneva

Wang RS, Wang R, Fraedrich K (1991) An approach to reconstruction of temperature on seasonal basis using historical documents from China. J Climatol 11: 381–392

Wang SW, Xie ZH, Cai JN, Zhu JH, Gong DY (2002) Global mean temperature during past 1000 years. Progress in Natural Sciences 12: 1145–1149

Yang HR, Xu X, Yang DY (1995) Environment changes and Geo-ecosystem of the lower Yangtze River. Nanjing: Press of Hohai University, pp 20–50 (In Chinese)

Zhang D, Liu C, Gu X (1996) A research of reconstruction of 6 regional dry/wetness grades series in the east China for the last 1000 years. In: Proceedings on the National Research Project (85–913) (eds) Collection of research papers on climate change and its numerical simulation (vol. 1). Beijing: Meteorological Press, pp 69–74 (in Chinese)

Zhang Q, Zhu C, Chen Ji (2002) Preliminary study on the flooding and drought calamity during past 1500 years in the Haian region. Chinese Geographical Science 12(2): 146–152

Zhang Q, Zhu C, Jiang FQ (2001) Environmental archaeological research of the Zhangjiangwan site of past 2000 years, Wushan, Chongqing, Acta Geographica Sinica 3: 353–362 (In Chinese)

Zheng SZ (1977) Changes of climatic humidity during past 2000 years in the South-eastern China. In: China Meteorological Agency (eds) Nanjing Institute of Geography and Limnology Collection of climatic changes and super-long prediction. Beijing: Science Press, pp 29–32 (In Chinese)

Authors' addresses: Tong Jiang, Qiang Zhang, Nanjing Institute of Geography and Limnology, Chinese Academy of Sciences (CAS), Nanjing 21008, China; Richard Blender, Klaus Fraedrich (e-mail: fraedrich@dkrz.de), Meteorologisches Institut, Universität Hamburg, 20146 Hamburg, Germany.